Indonesian Journal of Electrical Engineering and Computer Science
Vol. 25, No. 2, February 2022, pp. 741~754
ISSN: 2502-4752, DOI: 10.11591/ijeecs.v25.i2.pp741-754

Grid reactive voltage regulation and cost optimization for electric vehicle penetration in power network

Farrukh Nagi[1], Aidil Azwin[2], Navaamsini Boopalan[2], Agileswari K. Ramasamy[2], Marayati Marsadek[1], Syed Khaleel Ahmed[3]
[1]Institute of Power Engineering, Universiti Tenaga Nasional, Selangor, Malaysia
[2]Department of Electrical and Electronic Engineering, Universiti Tenaga Nasional, Selangor, Malaysia
[3]IEEE Signal Processing Society, Malaysia

Article Info

Article history:

Received Jul 16, 2021
Revised Dec 8, 2021
Accepted Dec 22, 2021

Keywords:

EV charging
GA optimization
Grid power and voltage control
IEEE33
Power analysis
Radial system
Reactive power injection

ABSTRACT

Expecting large electric vehicle (EV) usage in the future due to environmental issues, state subsidies, and incentives, the impact of EV charging on the power grid is required to be closely analyzed and studied for power quality, stability, and planning of infrastructure. When a large number of energy storage batteries are connected to the grid as a capacitive load the power factor of the power grid is inevitably reduced, causing power losses and voltage instability. In this work large-scale 18K EV charging model is implemented on IEEE 33 network. Optimization methods are described to search for the location of nodes that are affected most due to EV charging in terms of power losses and voltage instability of the network. Followed by optimized reactive power injection magnitude and time duration of reactive power at the identified nodes. It is shown that power losses are reduced and voltage stability is improved in the grid, which also complements the reduction in EV charging cost. The result will be useful for EV charging stations infrastructure planning, grid stabilization, and reducing EV charging costs.

Corresponding Author:

Navaamsini Boopalan
Department of Electrical and Electronic Engineering
University Tenaga Nasional, Jalan IKRAM-UNITEN, 43000 Kajang, Selangor, Malaysia
Email: navaamsini@gmail.com

Indices:

m EV index
n network node index
t timestamp index
j injection index

Variable Parameters:
ΔT Nodes reactive power injection duration (hr)
N Number of network nodes (n)
M Number of EVs per Node (m)
S Number of nodes for Injection(s)
E^{req} EV charge required (kWh)
t_{st} Start charging time variable (hr)
U_m Charging time variable EV (hr)

P_{avg} Average EV power constant (kW)
P^{ev} EV active power (kW)
$P^{ev,Loss}$ Active power loss due to EV (kW)
P^{Load} Other loads on network constant (kW)
S^{ev} App.arent EV power (kW)
Q^{ev} EV reactive power (kVar)
$Q^{ev,Loss}$ Reactive power loss due to EV (kVar)
V_L Network node voltage p.u.
V^{ev} EV voltage p.u.
$P^{x}_{n,t,m}$ EV Power charging variable (kW)
$\lambda_{n,t,m}$ EV charging cost constant
n^{sel} Optimized selected nodes
P^{ch} Maximum charging power rate for EV (kW)

Optimization Subscripts:
'^{uncoor}' Uncoordinated optimization
'^{coor}' coordinated optimization
'^{inj}' Reactive power injection optimization
'$^{inj,\ \Delta T}$' Reactive power injection optimization with time interval
'*' Optimized values
'^{Load}' Optimized values

Optimization Parameters:
'$^{?}$' *Below Replaces above Optimization Subscripts*
$E^{?}_{t}$ Network charge (kWh)
$P^{?}$ Network active power due to injection (kW)
$Q^{?}$ Network reactive power due to injection
$P^{?,Loss}$ Network active power loss due to injection (kW)
$Q^{?,Loss}$ Network reactive power loss due to injection (kVar)
$V^{?}$ Network voltage for duration ΔT p.u.
$P^{?,Loss}$ Network active power loss for duration ΔT (kW)
$Q^{?,Loss}$ Network reactive power loss for duration ΔT (kVar)
$f^{?}_{min}$ Optimization objective function
$\{P,Q\}^{?,?}$ Set of active and reactive power

1. INTRODUCTION

Reactive power compensation has been studied for many years with diversified research fields. The onset of renewable power sources and utilization brings new challenges for grid stabilization. As such EV load on the grid is expected to increase in the future which will aggravate electrical power supply stabilization and put forward new challenges to systems security, economics operation, and energy management. EV charging is subjective to the load on the bus network. EV charging stations and aggregators locations are selected on basis of lightly loaded nodes in the network buses.

On-load tap changer (OLTC) of the main transformer, switching of the substation, feeder capacitor banks [1], distributed generators (DG), and adjustable loads are integrated into distribution network [2] to overcome losses in network buses. The uncertainty of the large number of DG may lead to over voltage or under voltage, increasing the volatility of the voltage, as a result, the traditional distribution network is gradually changing over to the active distribution network (ADN). Kotenev *et al.* [3] present a mathematical model to control reactive voltage on a node by using the synchronous motor excitation control. Meng *et al.* [4] present a key node determination method to control reactive power and voltage optimization by compensation devices installed at the key nodes. Zechun and Mingming [5] choose the compensation nodes based on the sensitivity analysis. Whereas, in [6], the reactive power margins method is proposed to determine the nodes where reactive power compensators are installed. Distribution feeder configuration (DFR) is another way that reduces power losses and manages power stability in a power distribution system, by sectionalizing the network by closed switches and open tie loop switches. Singh and Tiwari [7] present a two-stage framework is proposed for real and reactive power management and DFR. Uncoordinated and random charging of EVs increases peak load, losses, and voltage limit violations in the distribution system

[8], [9]. The uncoordinated adverse EV charging effects can be removed by coordinated scheduling of EVs in which an aggregator coordinates their charging/discharging with the distribution system operator (DSO). The aggregator act as a business entity to schedule charging/discharging of EVs and address both interests of EV owners and DSO in terms of economic incentives and efficient system operation of power losses and voltage stabilization, respectively [10]-[14].

EV reactive voltage stabilization with grid injection problem is usually solved in phases. The demand decisions of each EV are managed by regional aggregators. The objective of each regional aggregator is to minimize net cost and load variations by solving an optimization problem to obtain an EV charging schedule. Based on the real power schedule of EVs, obtained from the first phase the regional aggregators determine the maximum aggregated reactive power that can be injected/absorbed by all EVs present at each node. This information associated with maximum reactive power injection/absorption of each node is sent to the DSO by each regional aggregator as shown in Figure 1. Thereafter, in the second stage, DSO performs simultaneous reactive power scheduling with power flow calculations to minimize losses in the distribution system. Wang *et al.* [15] presents coordinated EV charging with reactive power support to distribution grids at each network node. Shafiee *et al.* [16] investigate the impact of plug-in hybrid electric vehicles (HEV) on power distribution systems but didn't offer a solution for grid power losses. Modern inverters have the capability of providing reactive power support to improve voltage profiles and to minimize power, several authors have addressed this topic using the bi-directional EV battery charger enabled with the vehicle-to-grid (V2G) concept such as by Yong *et al.* [17]. The EV chargers also have the capability of allowing reactive power flow to the grid by utilizing the direct current (DC)-link capacitor.

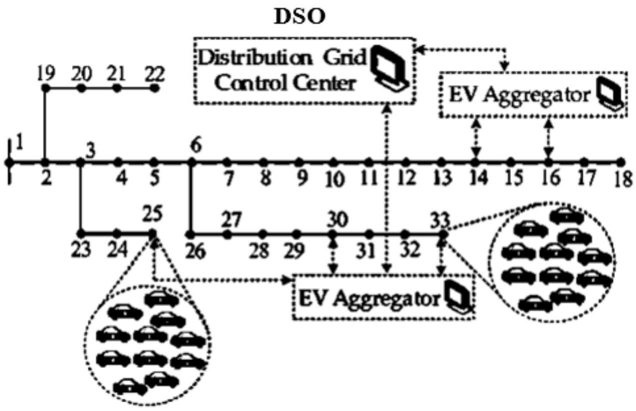

Figure 1. IEEE 33 node power network [15] connected with EV aggregator chargers and distributed grid control centre/DSO

The novel approach adopted in this work is to first search the network nodes which are most affected in the grid due to incoherent EV charging and then optimize the reactive power injection magnitude and time duration. Whereas all the research work mentioned above; studies the EV charging modeling and its impact on the grid and offers a solution to reduce the grid power losses by reactive power injection on all nodes irrespective of injection time duration. A large-scale 18K EV charging model is simulated in this work with driving pattern, EV charging intervals distributions, and EV charging cost. IEEE 33 node radial network [18], [19] is used for the study. This paper aims to regulate the grid voltage, and a new approach is considered here to minimize the EV charging voltage rather than the traditional minimization of the grid power losses approach. From an optimization point of view, the minimization decision criteria are based on the mean square error (MSE) of grid voltage while the input control variable is reactive injection power.

A sequence of numerical computations adopted in this work is described in sections 2-4. EV charging parameters are defined in section 2 and Table 1. EV user charging requirement is modeled with Weibull distribution in section 2.1. The daily demand profile and cost of electricity used in this study are discussed in section 2.2. In section 3.1 uncoordinated EV charging load without daily load, the profile is evaluated with B/F sweep power flow analysis. In section 3.2 the coordinated EV charging load and charging cost is optimized with load profile and charging constraints using mixed integer linear programming (MILP). In section 4 most affected power losses and voltage instability nodes are searched, followed by the optimization of reactive power injection magnitude required for its restoration. Finally, in section 5 the reactive power injection time duration is determined at the located nodes.

2. EV PARAMETERS AND CHARGING

IEEE 33 network [19] data in appendix 1 is used for simulation studies in this work. A large number of EVs=18000 are used in the simulation for maximum EV impact on the grid. Each node can act as an EV aggregator and can carry max $M = 563/node$ EVs with different state of charge (SoC) and random charging interval. Simulation studies are carried out for 24 hrs over 15 min time interval (96 time stamps).

2.1. EV charging distribution

Due to different brands of EV cars with battery energy capacities E_m^{req} ranges between 4kWh - 50kWh and considering local driving pattern the energy requirement probability is represented by the Weibull density [18] curve defined in (1).

$$f(E^{req}) = \frac{b}{a}.\left(\frac{E^{req}+c}{a}\right)^{b-1}.e^{-\left(\frac{E^{req}+c}{a}\right)^{b}} \tag{1}$$

Where choosing *a= 15, b= 1.4, c= 2*, the probability curve is given in Figure 2. Nominal average EV charging is considered as P_{avg} = 7.2kW. EV start charging times t_{st} are randomly generated based on local EV user charging behavior pattern shown in Figure 3 is based on 20% user charging between 07h00 - 10h30, 40% between 16h00-21h00, and the rest is evenly distributed over the day. The time interval U_m for mth EV is then random, both in start time t_{st} and energy required E_m^{req} and is defined by (2).

$$U_m = [t_{st}; stop\ time]$$

$$U_m = \left[t_{st}; t_{st} + \frac{E_m^{req}}{P_{avg}}\right] \tag{2}$$

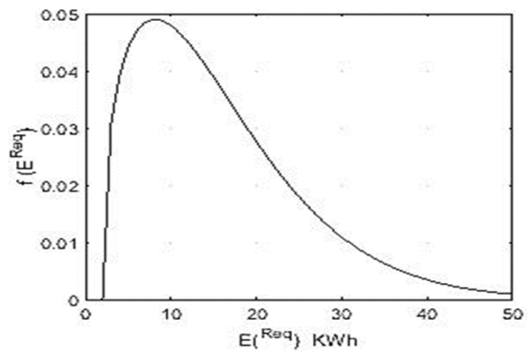

Figure 2. EV charging energy requirement is modeled with Weibull density probability

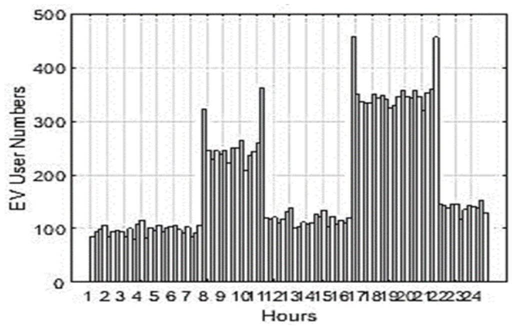

Figure 3. EV charging start time tst histogram

2.2. EV charging and network parameters

To simulate the EV charging process parameters in Table 1 are selected. General equatorial condition daily demand pattern and cost of electricity data used in this study are shown in Figure 4. The backward/forward sweep method [20] for power flow analysis is used for IEEE 33 radial distribution system shown in Figure 1. Baseload active and reactive power $(P,Q)_n^{Load}$, $(P,Q)_n^{Load,Loss}$ and voltage (V_L) p.u. of IEEE 33 radial system [19], is given in appendix 1.

Table 1. Network and EV parameters

Network PQ nodes, *N*	32
EV per node, *M*	563/node
Max EV charging Rate P_{ch}	9.4 kW
Average EV Charge P_{avg}	7.2 kW
Slack Gen PV node 1	5 MW
EV charger *PF*	0.74-0.98
Timestamp $\Delta t=15min$	96 min-step
Total EVs *(M . N)*	18,000
Base MVA	1000
Power factor, Phase Angle	0.74, -42.3o

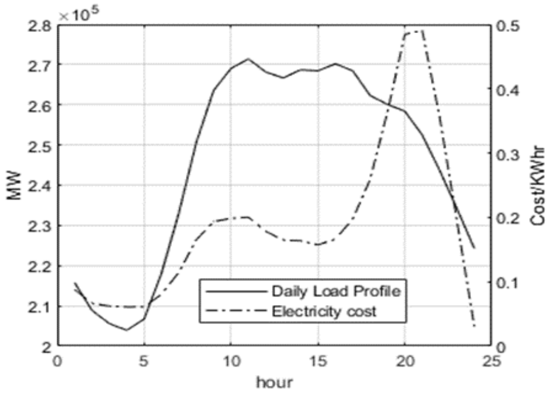

Figure 4. Daily load profile and cost of electricity

3. EV CHARGING

The high volume of EVs charging with the grid affects the grid voltage and power factor. The capacitive load of EV grid charging impacts the grid [21]. EV aggregator is expected to meet the demand of battery charging at an economical cost. EV power charging is modeled and simulated as a function of three variables EV number (*m*), Network node (*n*), and time (*t*).

3.1. Uncoordinated EV charging

For uncoordinated EV charging $E_{n,t,m}^{req}$ (kWh) is obtained from the Weibull distribution in (1) and charging interval $U_{n,t,m}$ is evaluated from (2). The EV charging power $P_{n,t}^{ev}$ required for all M=563/node on 32 nodes (N) for 15min time step *t* (1:96) is given in (3).

$$P_{n,t}^{ev} = \sum_{m}^{M=500} \frac{E_{n,t,m}^{req}}{U_{n,t,m}} \tag{3}$$

EV charger power factor [22] is varied between *pf* = [0.98: 0.74], *pf*=0.74 corresponds to a −42.3° angle between the voltage and current phasors. The *maximum* reactive voltage over *time* is shown in (4).

$$P_n^{uncoor} = \max_{t\in 96}[P_{n,t}^{ev}] \tag{4a}$$

$$S_n^{uncoor} = \left[\frac{P_n^{uncoor}}{pf_n}\right] \tag{4b}$$

$$Q_n^{uncoor} = \sqrt{S_n^{uncoor\,2} - P_n^{uncoor\,2}} \tag{4c}$$

3.2. Backward/forward sweep power flow

The backward/forward sweep method [16], [19] for power flow analysis is used for power flow analysis. Active power $P_n^{uncoor}$and reactive power Q_n^{uncoor} flows in a branch between node '*n*' to node '*n+1*', with branch resistance R_n and impedance X_n, given in appendix 1. B/F sweep method calculates backward from *(n+1)* node the last node (n) is given in (5) and (6).

$$P_n^{uncoor} = P_{n+1}^{uncoor\prime} + R_n \frac{P_{n+1}^{uncoor\prime 2} + Q_{n+1}^{uncoor\prime 2}}{V_{n+1,t}^2} \tag{5}$$

$$Q_n^{uncoor} = Q_{n+1}^{uncoor\prime} + X_n \frac{P_{n+1}^{uncoor\prime 2} + Q_{n+1}^{uncoor\prime 2}}{V_{n+1,t}^2} \tag{6}$$

Where the update values are, $P_{n+1}^{uncoor\prime} = P_{n+1}^{uncoor} + [P_{n+1}^{Load} + P_{n,t}^{ev}]$

$$Q_{n+1}^{uncoor\prime} = Q_{n+1}^{uncoor} + [Q_{n+1}^{Load} + Q_{n,t}^{ev}]$$

P_{n+1}^{Load} and Q_{n+1}^{Load} are IEEE 33 network loads in appendix 1, $P_{n,t}^{ev}$ and $Q_{n,t}^{ev}$ are the EV loads that are connected at node *'n+1'*. P_{n+1}^{uncoor} , Q_{n+1}^{uncoor} and V_{n+1}^2 are effective real, reactive power flows in network branches due to loads. The network node voltage is given in (7),

$$V_{n+1}^{uncoor} = V_n^{uncoor} - I_n \,.\, (R_n + jX_n) \tag{7}$$

Power Losses are shown in (8) and (9)

$$P_n^{uncoor,Loss} = I_n^2 * R_n \tag{8}$$

$$Q_n^{uncoor,Loss} = I_n^2 * jX_n \tag{9}$$

the voltage magnitude V_n^{uncoor} and the angle at each node are calculated in a forward direction and are used recursively in a forward direction to find the voltage and angle respectively of all nodes of radial distribution.

3.3. Coordinated EV charging with constraints and cost-MILP

The interest for the EV aggregator is to minimize the charging cost. Considering $P_{n,t,m}^x$ as decision variable for EV charging power, and $\lambda_{n,t,m}$ as charging cost. To optimize the EV charging load according to the charging cost and the load profile, the objective function f_{min}^{coor} minimize the product of EV charging power and cost of charging as (10),

$$f_{min}^{coor} = \sum_{\substack{1\le n\le N \\ 0\le t\le 96 \\ 0\le m\le M}} P_{n,t,m}^x \,.\, \lambda_{n,t,m} \tag{10}$$

subjected to constraint,

$$P_{n,t,m}^x \le P^{ch} \; (Max\ charging\ Limits) \tag{11}$$

$$P_{n,t,m}^x \le [P_{n,t,m}^{ev} + P_{n,t,m}^{Load}] \; (EV + Base\ Load) \tag{12}$$

$$P_{n,t,m}^x . U_{n,t,m} = E_{n,t,m}^{req} \; (Energ\ Balance) \tag{13}$$

$$P_{n,t,m}^x \ge 0 \tag{14}$$

constraints in (11), (14) are maximum charging power limit, optimized charging should be less than or equal to total inclusive of node load, optimized charging energy should be equal to required EV charging energy and positive charging power respectively.

Due to a large-scale optimization problem, IBM ILOG CPLEX optimization linear programming function '*cplexlp*' is used in MATLAB 2019 environment. For grid analysis, the maximum load value is considered at the node. Total nodes (*n*) load at $t + \Delta t$, where Δt *=15min*, is given in (15),

$$P_{n,t}^{coor} = \sum_{m}^{M=500} P_{n,t,m}^{ev^*} \therefore P_{n,t,m}^{ev^*} = P_{n,t,m}^{x^*} \quad (15)$$

where $P_{n,t,m}^{ev^*}$ is the coordinated optimized active power and $Q_{n,t,m}^{ev^*}$ can be found out similarly to (4). The *maximum* EV charging power at each *node* is defined in (16),

$$E_t^{coor} = \max_{\substack{M\in 500\\ N\in 32}} [P_{n,t,m}^{coor} \,.\, U_{n,t,m}] \quad (16)$$

the Backward/Forward sweep power flow analysis is used to evaluate the network nodes parameters,

$$P_n^{coor} = \max_{t\in 96} [P_{n,t}^{ev^*}] \quad (17a)$$

$$S_n^{coor} = \frac{P_n^{coor}}{pf_n} \quad (17b)$$

$$Q_n^{coor} = \sqrt{S_n^{coor\,2} - P_n^{coor\,2}} \quad (17c)$$

$$P_n^{coor} = P_{n+1}^{coor\prime} + R_n \frac{P_{n+1}^{coor\prime 2} + Q_{n+1}^{coor\prime 2}}{V_{n+1}^2} \quad (18)$$

$$Q_n^{coor} = Q_{n+1}^{coor\prime} + X_n \frac{P_{n+1}^{coor\prime 2} + Q_{n+1}^{coor\prime 2}}{V_{n+1}^2} \quad (19)$$

where,

$$P_{n+1}^{coor\prime} = P_n^{coor} + P_n^{Load}$$

$$Q_{n+1}^{coor\prime} = Q_n^{coor} + Q_n^{Load}$$

and,

$$V_{n+1}^{coor} = V_n^{coor} - I_n \,.\, (r_n + jX_n) \quad (20)$$

$$P_n^{cood,Loss} = I_n^2 \,.\, R_n \quad (21)$$

$$Q_n^{coor,Loss} = I_n^2 \,.\, jX_n \quad (22)$$

4. REACTIVE POWER INJECTION OPTIMIZATION-GA

Power losses and voltage stability can be improved with reactive power injection in (6). The optimized EV power $P_{n,t}^{ev^*}$ *(S)* nodes are searched here by GA to reduce power losses and stabilize the voltage. The reactive power may come from shunt capacitor bank, EV battery DC-link, or offload synchronous motor condenser. It is necessary to introduce injection power magnitude variable term $Q[j_{n'}]$ as a function of node location index $j_{n'}$ in (24) for mixed-integer GA optimizer as,

$$P_n^{inj} = \max_{t\in 96} [P_{n,t}^{ev^*}]$$

$$S_n^{inj} = \frac{P_n^{inj}}{pf_n}$$

$$Q_n^{inj} = \sqrt{S_n^{inj\,2} - P_n^{inj\,2}}$$

$$P_n^{inj} = P_{n+1}^{inj'} + R_n \frac{P_{n+1}^{inj'^2} + Q_{n+1}^{inj'^2}}{V_{n+1}^2} \quad (23)$$

$$Q_n^{inj} = Q[j_{n'}] + Q_{n+1}^{inj\prime} + X_n \frac{P_{n+1}^{inj\prime^2} + Q_{n+1}^{inj\prime^2}}{V_{n+1}^2} \tag{24}$$

where,

$$P_{n+1}^{inj\prime} = P_n^{inj} + P_n^{Load}$$

$$Q_{n+1}^{inj\prime} = Q_n^{inj} + Q_n^{Load}$$

and,

$$I_n^{inj} = \frac{Conj\left(P_n^{inj} + j.Q_n^{inj}\right)}{V_n^0} \tag{25a}$$

$$V_{n=1}^{inj} = 1\, p.u.$$

$$V_{n+1}^{inj} = V_n^{inj} - I_n^{inj}.(R_n + jX_n) \tag{25b}$$

$$P_n^{inj,Loss} = I_n^{inj^2}.R_n \tag{26}$$

$$Q_n^{inj,Loss} = I_n^{inj^2}.jX_n \tag{27}$$

the reactive power injection variable $Q[j_s]$ is defined as the customized function for 'Population Generation'. The index $s = 1{:}S$, are number nodes which optimizer will be searched to minimize the objective function (29). Selecting S=*3* sets the remaining *(32-S)* nodes are set to zero. $Q[j_s]$ denotes the reactive power injection magnitude variable, also searched by the mixed integer genetic algorithm (GA) optimizer.

$$j_s = randperm[\,0, 0, 0, 1_{n=4}, 0, 0, 1_{n=7}, \ldots 0, \ldots, 1_{n=17}, \ldots, 0]_{1x33} \tag{28a}$$

$$Q[j_s] = Q\begin{bmatrix} 0(1), 0(2), 0(3), Q[j_{4'}], 0(5), 0(6), Q[j_{7'}], \ldots \\ , 0(12), \ldots, Q[j_{17'}], \ldots, 0_{33} \end{bmatrix}_{1x33} \tag{28b}$$

The reactive power injection Q[j_s] is assigned a range of [0 300]KVar to minimize the objective function in (28)b. MATLAB command 'randperm' is a random and combinatorial set of cyclic permutations for GA optimization. Minimum voltage objective function is formed with two voltages, the constraint V_L IEEE base voltage p.u and variable term V_n^{inj} (25(b)) to represent the EVs charging voltage which is a function of $\boldsymbol{I_n^{inj}}$, P_n^{inj} and Q_n^{inj} in (23-27).

$$f_{min}^{inj} = \sqrt{[\textstyle\sum_n^N V_L]^2 + Max\left(V_n^{inj}\right)^2} \tag{29}$$

4.1. Reactive voltage injection time duration interval-GA

The optimized EV power $P_{n,t}^{ev^*}$ for S=3 nodes $n^{sel^*} = [14;\ 17;\ 18]_{3xl}$ selected in section 4 injects the reactive power over a 24 hour period which may not necessary for dynamic EV loads. To find optimal injection time interval (ΔT) hour and reduce injection charges at nodes $n^{sel^*} = [14;\ 17;\ 18]_{3xl}$, the optimization in section 4.0 is repeated with timestamp (t) variable and B/F sweep power flow analysis with time function is,

$$P_{n,t}^{inj,\Delta T} = P_{n,t}^{ev^*}$$

$$S_{n,t}^{inj,\Delta T} = \frac{P_{n,t}^{inj,\Delta T}}{pf_{n,t}}$$

$$Q_{n,t}^{inj,\Delta T} = \sqrt{S_{n,t}^{inj,\Delta T^2} - P_{n,t}^{inj,\Delta T^2}}$$

$$P_{n,t}^{inj,\Delta T} = P_{n+1,t}^{inj,\Delta T\prime} + R_n \frac{P_{n+1,t}^{inj,\Delta T\prime^2} + Q_{n+1,t}^{inj,\Delta T\prime^2}}{V_{n+1,t}^2} \quad (30)$$

$$Q_{n,t}^{inj,\Delta T} = inj_{t,n^{sel*}} + Q_{n+1,t}^{inj,\Delta T\prime} + X_n \frac{P_{n+1,t}^{inj,\Delta T\prime^2} + Q_{n+1,t}^{inj,\Delta T\prime^2}}{V_{n+1,t}^2} \quad (31)$$

where the updates with time function (t) are,

$$P_{n+1,t}^{inj,\Delta T\prime} = P_{n,t}^{inj,\Delta T} + P_{n,t}^{Load}$$

$$Q_{n+1,t}^{inj,\Delta T\prime} = Q_{n,t}^{inj,\Delta T} + Q_{n,t}^{Load}$$

using GA MILP optimization with customized random *'PopulationGeneration'* hourly timestamp is randomly searched over 24 hours in three nodes n_{sel} defined as,

$$inj_{t,n}^{sel} = rand \begin{bmatrix} 0_1\,0_2\,1_3 & \cdots & 0_{24} \\ 1_1\,0_2\,0_3 & \cdots & 0_{24} \\ 0_1\,0_2\,0_3 & \cdots & 1_{24} \end{bmatrix} \begin{bmatrix} 242 \\ 224 \\ 102 \end{bmatrix}$$

and,

$$V_{n+1,t}^{inj,\Delta T} = V_{n,t}^{inj,\Delta T} - I_{n,t} \,.\left(R_{n,t} + jX_{n,t}\right) \quad (32)$$

$$P_{n,t}^{inj,\Delta T,Loss} = I_{n,t}^{inj,\Delta T^2} \,.R_{n,t} \quad (33)$$

$$Q_{n,t}^{inj,\Delta T,Loss} = I_{n,t}^{inj,\Delta T^2} \,.jX_{n,t} \quad (34)$$

the Objective function is defined as before in (29) with an additional time interval *(t)* variable to determine the reactive power injection $Q[\,n^{sel^*}]^*$. The minimum time interval for the selected nodes $n^{sel^*} = [14;\ 17;\ 18]_{3xl}$.

$$f_{min}^{inj,\Delta T} = \sqrt{\sum_n^N V_L{}^2 + Max\left(V_{n,t}^{inj,\Delta T}\right)^2} \quad (35)$$

5. RESULTS

Coordinated power EV charging P_n^{coor} and 1hr injection EV charging power $P_n^{inj,\Delta T}$ are shown in Figure 5, with higher power utilization at lower daily demand and electricity rates. Uncoordinated [23] EV charging the penetration to the grid starts immediately when the user arrives at home and plug-in. Most EV users arrive at home at the same period of peak demand creating a large load, power losses increased 10 times as shown in Figures 6-7, and voltage instability increases in Figure 8. Coordinated charging with the objective function f_{min}^{coor} and constraints of variable $P_{n,t,m}^{x}$ in (11) and (14) reduces the network power losses $P_n^{coor,Loss}$, $Q_n^{coor,Loss}$ in Figures 6-7 and stabilize the voltage V_n^{coor} in Figure 7. GA optimization with the objective function f_{min}^{inj} for power losses $P_n^{inj,Loss}$, $Q_n^{inj,Loss}$ and voltage drop V_n^{inj} which randomly search j_s nodes for 24hr reactive power injection results in selected nodes $j_s^* = [n^{sel^*}]_{3x1}$ are shown in Table 2. The GA optimization objective function $f_{min}^{inj,\Delta T}$ for 1hr reactive power injection results in $P_n^{inj,\Delta T,Loss}$, $Q_n^{inj,\Delta T,Loss}$, $V_n^{inj,\Delta T^*}$ further reduces the active and reactive power in Figures 6-7.

Table 2. Three node injection

Inj. Voltage	Inj. Hr
$Q[\,n^{sel^*}]^*$	$j_{t,n^{sel^*}}$
242	1
224	1
102	18

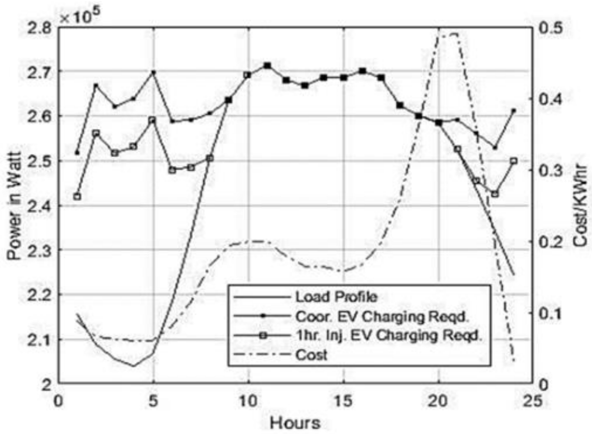

Figure 5. Daily load profile and cost of electricity. Shows the excess EV charging power required in 1-7hr with coordinated and 1hr reactive power injection

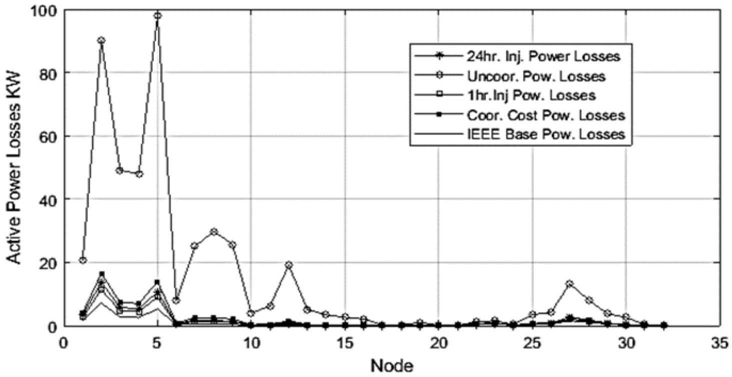

Figure 6. Active power losses P_{n+1}^{Load}, $P_n^{coor,Loss}$, $P_n^{uncoor,Loss}$, $P_n^{inj,Loss}$ and $P_n^{inj,\Delta T,Loss}$

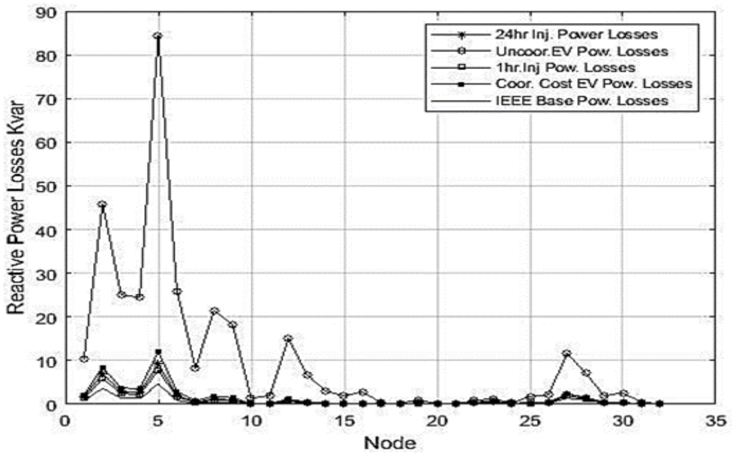

Figure 7. Reactive power losses Q_{n+1}^{Load}, $Q_n^{coor,Loss}$, $Q_n^{uncoor,Loss}$, $Q_n^{inj,Loss}$ and $Q_n^{inj,\Delta T,Loss}$

It is observed that 1hr injection traces closely matched with IEEE Base network traces. Active and reactive power losses of IEEE baseload $\{P,Q\}_n^{Load,Loss}$,$\{P,Q\}_n^{coor,Loss}$,$\{P,Q\}_n^{uncoor,Loss}$, 24hr reaction power injection $\{P,Q\}_n^{inj,Loss}$ and 1hr reaction power injection $\{P,Q\}_n^{inj,\Delta T,Loss}$ are shown in Figures 6-7.

IEEE network p.u. voltage V_L, V_n^{coor} , V_n^{uncoor} ,$V_{n,t}^{inj}$ and $V_{n,t}^{inj,\Delta T}$ are shown in Figure 8. 1hr voltage trace is the most stable voltage matching with IEEE network voltage V_L. Table 3 summarizes the comparative results of the techniques used in this research work.

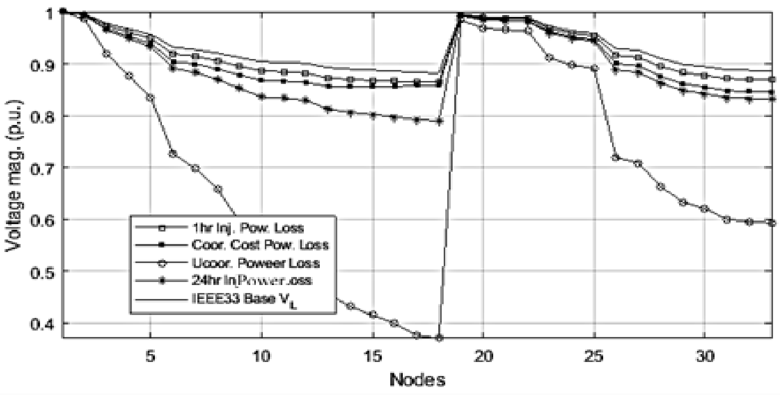

Figure 8. Nodes voltages p.u. VL, V_n^{coor} , V_n^{uncoor} ,$V_{n,t}^{inj}$ and $V_{n,t}^{inj,\Delta T}$

Table 3. Results of techniques used

Analysis	Sum of Active Power Losses (kW)	Sum of Reactive Power Losses (kVar)	Voltage MSE
Uncoordinated EV Charging	477.72	329.06	7.6568
Coordinated EV Charging	69.51	46.62	0.7993
24 hr. Injection EV Charging	56.04	37.53	1.4417
1 hr. Injection EV Charging	46.02	30.77	0.3952
IEEE Base load without EV	28.15	18.79	0

Despite stabilizing the grid voltage and improving power losses at the most affected nodes. The optimized power injection magnitude has the drawback of requiring all the nodes to be equipped to inject reactive voltage back V2G into the grid. This technique is efficient for known injection nodes at the hot spot (commercial outlets, offices, restaurants) injection nodes [24], [25] and equipped with reactive voltage injection devices.

6. CONCLUSION

A large number of EVs charging with the grid affects the grid voltage and power factor. EV grid charging impacts the grid with capacitive load. In this paper, the grid voltage recovery is demonstrated for 18K EVs charging load due to load profile capacity. It is shown that optimized reactive power injection magnitude and time interval at the most affected nodes stabilize the grid voltage and improve power losses. Changing EV's user driving pattern distribution, cost (λ), and local load profile, will help to locate the installation of EV charging stations and the aggregators to inject reactive power for power stability. EV charging analysis presented in this work can be extended and compared with distribution Feeder reconfiguration (DFR) of the IEEE network to study the grid stabilization problem. Further, the number of EVs can be increased and analyzed with higher profile loads.

APPENDIX

IEEE 33 BUS DATA

Line Number	Sending Bus	Receiving Bus	Resistance (Ω)	Reactance (Ω)	Load at receiving end Bus Real Power (kW)	Load at receiving end Bus Reactive Power (kVAr)	$P_n^{Load\ Loss}$ (kW)	$Q_n^{Load\ Loss}$ (kW)
1	1	2	0.0922	0.0477	100.0	60.0	16.80	8.57
2	2	3	0.4930	0.2511	90.0	40.0	71.39	36.36
3	3	4	0.3660	0.1864	120.0	80.0	27.67	14.09
4	4	5	0.3811	0.1941	60.0	30.0	26.04	13.26

IEEE 33 BUS DATA (cont.)

Line Number	Sending Bus	Receiving Bus	Resistance (Ω)	Reactance (Ω)	Load at Receiving End Bus Real Power (kW)	Load at Receiving End Bus Reactive Power (kVAr)	$P_n^{Load\ Loss}$ (kW)	$Q_n^{Load\ Loss}$ (kW)
5	5	6	0.8190	0.7070	60.0	20.0	53.30	46.01
6	6	7	0.1872	0.6188	200.0	100.0	2.68	8.85
7	7	8	1.7114	1.2351	200.0	100.0	6.79	2.24
8	8	9	1.0300	0.7400	60.0	20.0	5.89	4.23
9	9	10	1.0400	0.7400	60.0	20.0	5.02	3.56
10	10	11	0.1966	0.0650	45.0	30.0	0.78	0.26
11	11	12	0.3744	0.1238	60.0	35.0	1.24	0.41
12	12	13	1.4680	1.1550	60.0	35.0	3.77	2.97
13	13	14	0.5416	0.7129	120.0	80.0	1.03	1.36
14	14	15	0.5910	0.5260	60.0	10.0	0.51	0.45
15	15	16	0.7463	0.5450	60.0	20.0	0.40	0.29
16	16	17	1.2890	1.7210	60.0	20.0	0.36	0.48
17	17	18	0.7320	0.5740	90.0	40.0	0.08	0.06
18	18	19	0.1640	0.1565	90.0	40.0	0.21	0.20
19	19	20	1.5042	1.3554	90.0	40.0	1.11	1.00
20	20	21	0.4095	0.4784	90.0	40.0	0.13	0.16
21	21	22	0.7089	0.9373	90.0	40.0	0.06	0.08
22	22	23	0.4512	0.3083	90.0	50.0	4.30	2.94
23	23	24	0.8980	0.7091	420.0	200.0	6.96	5.49
24	24	25	0.8960	0.7011	420.0	200.0	1.74	1.36
25	25	26	0.2030	0.1034	60.0	25.0	3.65	1.86
26	26	27	0.2842	0.1447	60.0	25.0	4.68	2.38
27	27	28	1.0590	0.9337	60.0	20.0	15.90	14.02
28	28	29	0.8042	0.7006	120.0	70.0	11.03	9.61
29	29	30	0.5075	0.2585	200.0	600.0	5.49	2.80
30	30	31	0.9744	0.9630	150.0	70.0	2.25	2.23
31	31	32	0.3105	0.3619	210.0	100.0	0.30	0.35
32	32	33	0.3410	0.5302	60.0	40.0	0.02	0.03

ACKNOWLEDGEMENTS

The optimization part of this project was developed as the outcome of UNITEN BOLD Project Code: RJO10517844/065. The Processing fee is funded by BOLD Research Grant code: J510050002/3032064.

REFERENCES

[1] Y. W. Li, "Smart grid and its application," *Adv. Mater. Res.*, vol. 986-987, no. June, pp. 533-536, 2014, doi: 10.4028/www.scientific.net/AMR.986-987.533.
[2] H. E. Farag, E. F. El-Saadany, and R. Seethapathy, "The Evolution for Voltage and Reactive Power Control in Smart Distribution Systems," *Int. J. Emerg. Electr. Power Syst.*, vol. 13, no. 1, 2012, doi: 10.1515/1553-779x.2772.
[3] V. I. Kotenev, V. V. Kochetkov, and D. A. Elkin, "The reactive power control of the power system load node at the voltage instability of the power supply," in *2017 International Siberian Conference on Control and Communications, SIBCON 2017 - Proceedings*, 2017, pp. 3-6, doi: 10.1109/SIBCON.2017.7998498.
[4] Q. Meng, R. Che, and S. Gao, "Reactive Power and Voltage Optimization Control Strategy in Active Distribution Network Based on the Determination of the Key Nodes," in *IOP Conference Series: Materials Science and Engineering*, 2017, vol. 199, no. 1, pp. 1-6, doi: 10.1088/1757-899X/199/1/012101.
[5] H. Zechun and Z. Mingming, "Optimal Reactive Power Compensation for Medium and Low Voltage Distribution Network Considering Multiple Load Levels," *Trans. China Electrotech. Soc.*, vol. 25, no. 8, pp. 167-172, 2010.
[6] L. C.-quan and Z. Yan, "Confirmation of Reactive Power Compensation Node and Its Optimal Compensation Capacity," *Power Syst. Technol.*, vol. 31, pp. 78-81, 2007.
[7] J. Singh and R. Tiwari, "Electric Vehicles Reactive Power Management and Reconfiguration of Distribution System to Minimize Losses," *IET Gener. Transm. Distrib.*, vol. 14, no. 25, pp. 6285 - 6293, 2020, doi: 10.1049/iet-gtd.2020.0375.
[8] K. C.-Nyns, E. Haesen, and J. Driesen, "The impact of Charging plug-in hybrid electric vehicles on a residential distribution grid," *IEEE Trans. Power Syst.*, vol. 25, no. 1, pp. 371-380, 2010, doi: 10.1109/TPWRS.2009.2036481.
[9] S. Shafiee, M. F.-Firuzabad, and M. Rastegar, "Investigating the impacts of plug-in hybrid electric vehicles on distribution congestion," *IET Conf. Publ.*, vol. 2013, no. 615 CP, pp. 1-10, 2013, doi: 10.1049/cp.2013.0596.
[10] Y. He, B. Venkatesh, and L. Guan, "Optimal scheduling for charging and discharging of electric vehicles," *IEEE Trans. Smart Grid*, vol. 3, no. 3, pp. 1095-1105, 2012, doi: 10.1109/TSG.2011.2173507.
[11] S. Han, S. Han, and K. Sezaki, "Development of an optimal vehicle-to-grid aggregator for frequency regulation," *IEEE Trans. Smart Grid*, vol. 1, no. 1, pp. 65-72, 2010, doi: 10.1109/TSG.2010.2045163.
[12] J. Wang, "*Active and Reactive Power Control of Flexible Loads for Distribution-Level Grid Services*," Michigan Technological University, 2018.
[13] S. Huang, J. R. Pillai, B. Bak-Jensen, and P. Thøgersen, "Voltage support from electric vehicles in distribution grid," *2013 15th European Conference on Power Electronics and Applications (EPE)*, 2013, doi: 10.1109/EPE.2013.6634344.
[14] J. Tomić and W. Kempton, "Using fleets of electric-drive vehicles for grid support," *J. Power Sources*, vol. 168, no. 2, pp. 459-468, 2007, doi: 10.1016/j.jpowsour.2007.03.010.

[15] J. Wang, G. R. Bharati, S. Paudyal, O. Ceylan, B. P. Bhattarai, and K. S. Myers, "Coordinated Electric Vehicle Charging With Reactive Power Support to Distribution Grids," *IEEE Trans. Ind. Informatics*, vol. 15, no. 1, pp. 54-63, 2019, doi: 10.1109/TII.2018.2829710.

[16] S. Shafiee, M. F.-Firuzabad, and M. Rastegar, "Investigating the Impacts of Plug-in Hybrid Electric Vehicles on Power Distribution Systems," *IEEE Trans. Smart Grid*, vol. 4, no. 3, pp. 1351-1360, 2013, doi: 10.1109/TSG.2013.2251483.

[17] J. Y. Yong, V. K. Ramachandaramurthy, K. M. Tan, and N. Mithulananthan, "Bi-directional electric vehicle fast charging station with novel reactive power compensation for voltage regulation," *Int. J. Electr. Power Energy Syst.*, vol. 64, pp. 300-310, 2015, doi: 10.1016/j.ijepes.2014.07.025.

[18] M. Baran and F. Wu, "Network Reconfiguration in Distribution Systems for Loss Reduction and Load Balancing," *IEEE Trans. Power Deliv.*, vol. 4, no. 2, pp. 1401-1407, 1989, doi: 10.1109/61.25627.

[19] J. Ponoćko, "Data Analytics-Based Demand Profiling and Advanced Demand Side Management for Flexible Operation of Sustainable Power Networks," in *Springer*, 2020, pp. 191-197, doi: 10.1007/978-3-030-39943-6.

[20] J. A. M. Rupa and S. Ganesh, "Power flow analysis for radial distribution system Using Backward/Forward Sweep Method," *Int. J. Electr. Comput. Energ. Electron. Commun. Eng.*, vol. 8, no. 10, pp. 1621-1625, 2014, doi: 10.5281/zenodo.1337731.

[21] M. Lillebo, S. Zaferanlouei, A. Zecchino, and H. Farahmand, "Impact of large-scale EV integration and fast chargers in a Norwegian LV grid," *J. Eng.*, vol. 2019, no. 18, pp. 5104-5108, 2019, doi: 10.1049/joe.2018.9318.

[22] A. R. Abul'Wafa, A. E' Garablyl, and W. A. F. Mohamed, "Uncoordinated vs Coordinated Charging of Electric Vehicles in Distribution Systems Performance," *Int. J. Eng. Inf. Syst.*, vol. 1, no. 6, pp. 54-65, 2017, [Online]. Available: www.ijeais.org54

[23] J. M. Clairand, J. R. Garcia, and C. A. Bel, "Smart charging for an electric vehicle aggregator considering user tariff preference," in *2017 IEEE Power and Energy Society Innovative Smart Grid Technologies Conference, ISGT 2017*, 2017, pp. 1-5, doi: 10.1109/ISGT.2017.8086068.

[24] C. Karolemeas, S. Tsigdinos, P. G. Tzouras, A. Nikitas, and E. Bakogiannis, "Determining electric vehicle charging station location suitability: A qualitative study of greek stakeholders employing thematic analysis and analytical hierarchy process," *Sustainability*, vol. 13, no. 4, pp. 1-21, 2021, doi: 10.3390/su13042298.

[25] M. Carrión, R. Zárate-Miñano, and R. Domínguez, "Integration of electric vehicles in low-voltage distribution networks considering voltage management," *Energies*, vol. 13, no. 6, pp. 1-23, 2020, doi: 10.3390/en13164125.

BIOGRAPHIES OF AUTHORS

Dr. Farrukh Nagi is a retd professor from Universiti Tenaga Nasional, department of mechanical engineering. Graduated from NED engineering university, Karachi (1982). Completed his MS from the University of Miami USA (1989) and his PhD from the University of Nottingham UK (1993). Since 2000 has been working on optimization, fuzzy control, and neural network systems. His current interest includes EV charging, Design, and development of Power industry safety devices, Artificial Intelligence tools for industrial maintenance. He can be contacted at email: farrukh@uniten.edu.my.

Aidil Azwin Bin Zainul Abidin received his BSEE from Indiana University Perdue University Indianapolis in 1999. He then obtained his Masters in Electrical Power from Universiti Tenaga Nasional in 2005. In 2012 he received his PhD in Engineering from Universiti Tenaga Nasional. His research interest includes Power System Simulations, Real-Time Simulations, Power System Protection, and Applied Artificial Intelligence. He can be contacted at email: AidilAzwin@uniten.edu.my.

Navaamsini Boopalan graduated from University Tenaga Nasional (UNITEN) with a bachelor's degree in electrical and electronic engineering. She has completed her M.Eng in Electrical Engineering at UNITEN in 2017. She is currently doing her PhD at the same institution. Her research focuses on optimization, signal and systems processing. She can be contacted at email: navaamsini@gmail.com.

Agileswari K. Ramasamy has obtained her B.Sc. (Engineering) degree from Purdue University in the United States in 1995. She received her MSc. (Control System) from Imperial College, London, and a PhD in Electrical Engineering from Universiti Tenaga Nasional. She is presently a Professor in UNITEN's Department of Electronics and Communication Engineering, and the Deputy Dean of Research and Postgraduate for the College of Engineering. She is actively involved in control systems, power systems, power quality, energy efficiency, and renewable energy research and consulting. She can be contacted at email: agileswari@uniten.edu.my.

Marayati Binti Marsadek graduated from The National Energy University in Putrajaya, Malaysia, with a Bachelor of Electric Power and a Master of Electrical Engineering in 2002 and 2006, respectively. In 2011, she received a PhD in Electrical, Electronics, and System Engineering from Malaysia's National University. She is the Director of the Institute of Power Engineering and a Senior Lecturer at Malaysia's National Energy University's Department of Electric Power. Power system stability, active network management, and risk assessment are among her research interests. She can be contacted at email: marayati@uniten.edu.my.

Syed Khaleel Ahmed is a consultant and mentor. He has graduated with B.E. in Electrical and Electronics Engineering from Anna University's College of Engineering, Guindy, in Chennai, India, and an M.S. in Electrical and Computer Engineering from the University of Massachusetts at Amherst in the United States. He has over 30 years of experience in industry and academics. His areas of specialization are Robust Control, Signal & Image Processing, and Application of Numerical Techniques. He is an ardent user and promoter of open-source software. He can be contacted at email: syedkhaleel2000@gmail.com.
.